Concept level evaluation of the full-scale deployment of fibre Bragg grating sensors for measuring forces in JET during plasma disruption events

P. Niewczas[1], G. Fusiek[1], C. Lescure[2], M. Johnson[2], E. Ivings[2], A. West[2], P. Crolla[1], M. Walsh[2]

JET-EFDA, Culham Science Centre, Abingdon, OX14 3DB UK

[1]Institute for Energy and Environment, Department of Electronic and Electrical Engineering, University of Strathclyde, 204 George Street, Glasgow, G1 1XW, UK
Tel: +44 (0)141 548 2869; Email: p.niewczas@strath.ac.uk

[2]EURATOM/UKAEA Fusion Association, Culham Science Centre, Abington, Oxon, OX14 3DB, UK

Abstract

In this paper we investigate the possibility of using fibre Bragg grating sensors to measure dynamic forces acting on vessel restraints in the JET (Joint European Torus) machine during plasma disruption events. The JET vacuum vessel consists of eight segments ("octants"), each having four legs, two on top and two on the bottom. At present, the measurement is performed using foil strain gauges mounted directly on each of the 32 legs. During a disruption event a thermal quench occurs followed by a current quench "CQ". The rapidly changing plasma current and position during the CQ results in considerable forces being exerted on the vacuum vessel due to electromagnetic interaction. Therefore, accurate monitoring of the forces is essential so that the machine control parameters can be adjusted appropriately for any experimental campaign. However, during plasma disruption events, the measurement using conventional gauges is compromised by the excessive noise induced in the instrumentation wires due to extreme electromagnetic interference. Moreover, after the installation of the divertor coils on JET, force measurements on the top and the bottom restraints are found to be different. This discrepancy is not fully understood, and so it is desirable to install an alternative measurement system, immune to electromagnetic interference so that the present measurement data could be corroborated with potentially more accurate optical measurements.

Based on a small-scale trial, the results of which are reported here, we investigate the range of technical problems that need to be addressed before a full-scale system can be realised. One problem area is associated with the sensor deployment, including the mounting procedures, sensor ruggedisation, fault tolerance and the predicted environmental impact on sensor performance. Another problem area is associated with the sensor interrogation system, including the realisation of a system capable of interrogating at least 32 sensors simultaneously; the accomplishment of acceptable measurement frequency, resolution and accuracy; and appropriate interfacing with the JET control system. A range of most promising solutions will be critically assessed and recommendations will be made for the deployment of the most optimal measurement system achievable with the current state of the art in fibre-optic sensing.

1. Introduction

In 1984, sixty-four strain gauges were mounted on the JET machine supports. Until 1997 only thirty-two were used for monitoring purposes. With the upgrade of the Torus Protection System (TPS) within the Machine Diagnostic System all sixty-four were integrated into the data bus. The purpose of the strain system is to determine strain changes (forces) in the vessel during temperature variations and operation.

The present measurement scheme uses foil strain gauges. During normal operation they are sampled at a rate of 25 Hz, and during disruptions the sampling rate is increased to 2.5 kHz. Furthermore, to reduce the influence of electromagnetic interference, a 5 kHz carrier signal is used. The instrumentation signals are integrated into JET's Control and Data Acquisition System (CODAS) via the Machine Diagnostic System (MDS). The gauges are in a "Full Bridge" configuration with no cable resistance compensation system, which prevents the system "zeroing" for calibration purposes [5].

To our knowledge, the application of fibre Bragg gratings (FBG) for monitoring the dynamic strain in Tokamak environment has not been reported so far. However, the testing of fibre Bragg gratings as temperature sensors in nuclear fission environment has been reported in literature. For example, a maximum of 5°C error was recorded after 600 MGy of gamma irradiation and 2×10^{19} n cm^{-2} neutron fluence [3]. One long-term study found a maximum 3°C error in temperature measurements after 50 months with a total gamma irradiation of 3.8 MGy and a total neutron fluence of 9.9×10^{17} n cm^{-2} (thermal, epithermal and fast) [4]. (Note that 1°C error is equivalent to approximately 10 με.) Furthermore, an investigation into the effects of radiation from JET plasma on fibres was undertaken as part of the 2003 deuterium-tritium campaign [6]. This investigation allowed the effects of ~14 MeV neutrons on optical fibres carrying visible wavelengths to be studied. 6% attenuation in visible wavelength transmission power was attributed to the neutron-gamma radiation flux. However, the FBG system under consideration operates around the telecoms C and/or L bands, and so these studies may not be relevant in this case.

Section 2 reports on the small-scale trial concerning the installation of four FBG sensors on four individual JET vessel restraints and their testing under various plasma disruption conditions between 19 March and 1 April 2008. Following this, the critical aspects of a full-scale deployment is analysed briefly in Section 3.

2. Small-scale trial

The limited extent of this trial allowed for the installation of four FBG sensors, used with an interrogation system developed previously for dynamic interrogation of FBG sensors [1]. Details of the measurement system, sensor installation and test results are presented below.

2.1 Measurement system overview

A schematic diagram of the FBG measurement system deployed at JET is shown in Figure 1 below. A superfluorescent light source (SFS), providing up to 30 mW of continuous power in the telecoms C-Band was employed by the interrogator. The source was used to illuminate 4 FBG sensors via an optical coupler and two separate 80-m fibre-optic cables. The cables contained multiple fibres, but only one fibre per line was used in this trial. Two fibre-optic connection boxes were also mounted for convenient

connecting of the sensors, one at the bottom and one near the top of the JET machine (not shown in Figure 1).

The wavelength encoded signals returned from the FBGs were mixed in the coupler and analysed using a tunable Fabry-Perot filter. The filter was driven using a saw-tooth signal to allow repeatable scanning over the required bands. To increase the scanning speed, detailed scanning was performed around the FBG peaks and coarse scanning outside the spectral regions of interest. The details of such selective scanning are given elsewhere [1]. The optical power at the scanning filter output was converted to an electrical signal using a photoreceiver module. The electrical signal was then analysed using a National Instruments PXI system, and the peak wavelengths returned by the FBGs could be observed on the screen and recorded following the reception of a digital trigger signal from CODAS. A double-line peak detection technique was used to recover FBG peaks [1]. Using the selective scanning technique, the acquisition rate of 1.6 kS/s for all the four FBGs was achieved. At this scanning frequency and the achieved power budget, the resolution was below ±2με for the bottom FBGs and the top-right FBG. The top-left FBG had a faulty pigtail splice, which resulted in poorer resolution, which amounted to approximately ±6με.

The interrogation system was placed outside the biological shield, some 80 m away from the sensors.

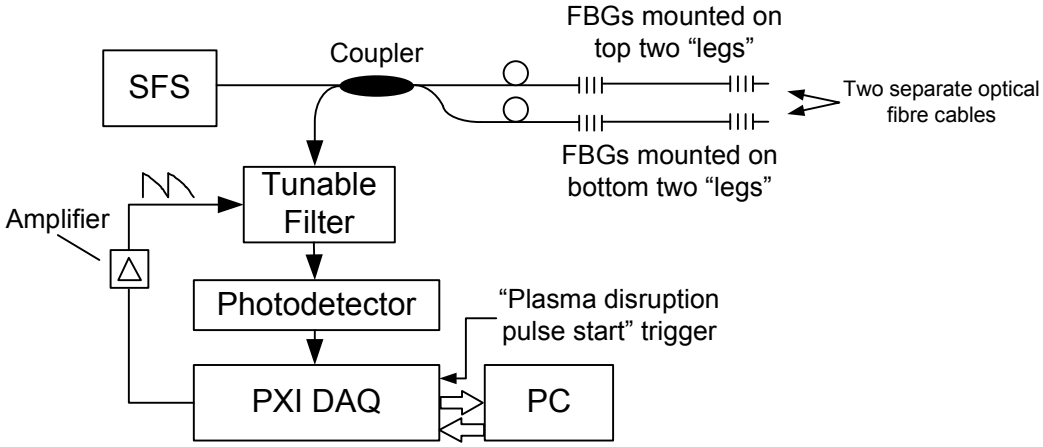

Figure 1. Schematic diagram of the FBG measurement system deployed on JET.

2.2 Sensor deployment

As highlighted above, 4 FBG sensors were deployed. Two sensors were mounted on the two top restraints and the other two sensors on the two bottom restraints of Octant 6. Strain gauge cement was used to attach the sensors to bare polished surfaces, prepared a few days before installation (see Figure 2). As shown in Figure 2, the FBGs were protected using metal boxes which were clamped to the vessel restraints. Optical connectors were mounted on side walls of the boxes to enable connecting the FBGs to the addressing fibres. The installation of four FBGs was carried out over 4-5 hours. The fibre-optic cables and connection boxes were installed beforehand.

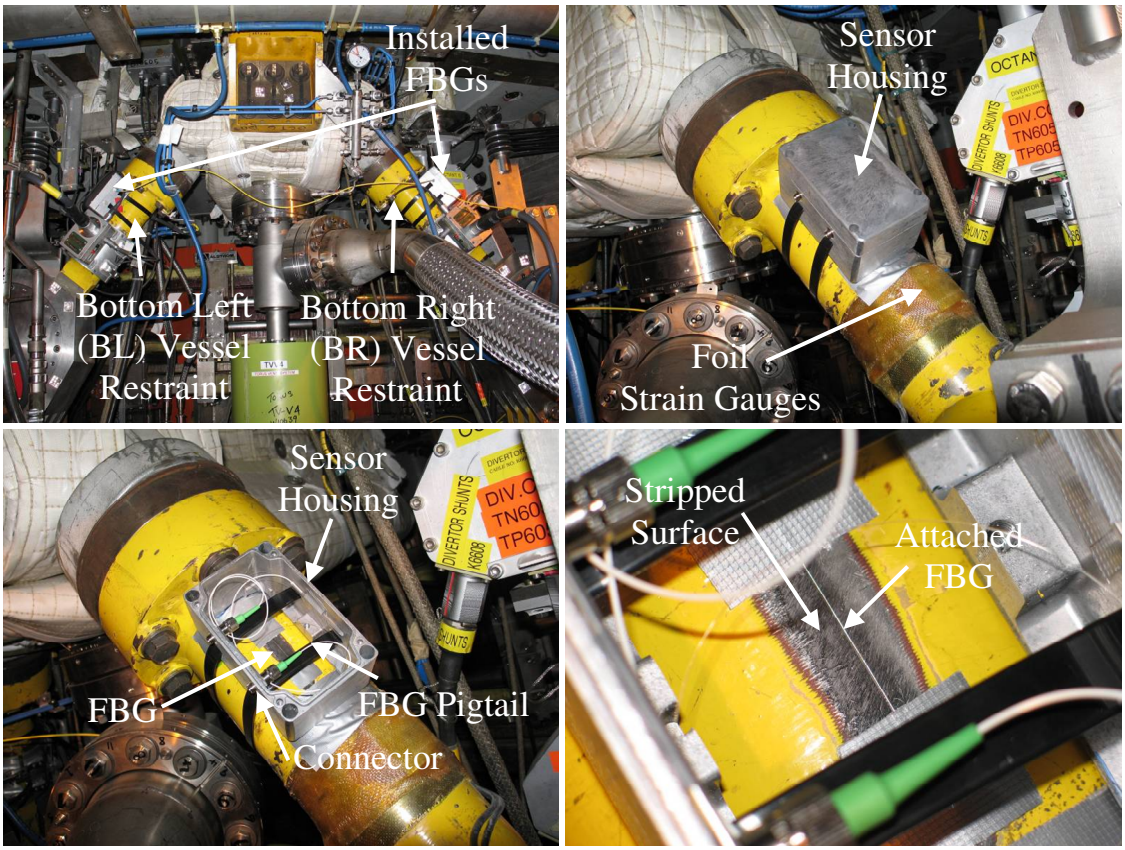

Figure 2. Photographs illustrating the positioning of the FBG sensors with respect of the vessel restraints and an internal sensor arrangement.

2.3 Test results and discussion

As highlighted in the introduction, the principal objectives of the trial were to corroborate the readings from the existing strain gauges and to provide a practical demonstration of the FBG measurement system in the tokamak environment.

The FBG interrogation system was configured to accept an external "master" trigger from the JET control system, which occurred during the pulse start. However, both pre- and post-trigger events were recorded in order to obtain the full picture of strain evolution in the monitored JET restraints. The recorded signals were post-processed by converting the individual FBG peak wavelengths into strain. This was achieved using the following formula [2]:

$$\frac{\Delta\lambda_B}{\lambda_B} = \left[1 - \frac{n_{eff}^2}{2}\left((1-\nu)\rho_{12} - \nu\rho_{11}\right)\right]\Delta\varepsilon = \left[1-\rho_e\right]\Delta\varepsilon = 0.782\cdot\Delta\varepsilon\,, \qquad (1)$$

where λ_B and $\Delta\lambda_B$ are the Bragg wavelength at ambient temperature and wavelength change due to straining, respectively; n_{eff} is the effective refractive index of the fibre core (n_{eff} = 1.465 for the germanium-doped core); ν is Poisson's ratio of silica glass (0.17); ρ_{11} and ρ_{12} are the photoelastic coefficients (values of 0.121 and 0.270, respectively); $\Delta\varepsilon$ is the strain change in $\mu\varepsilon$; and ρ_e is the stress-optic coefficient.

The FBG strain data was then compared with that recorded from the foil strain gauges. As highlighted before, there were two foil strain gauges originally mounted on each restraint. Strain data from several disruption events was then collated and plotted for

comparison. Plots of the complete set of data from Pulse 71990, representing a 164-ton plasma disruption, are shown in Figures 3 to 8. Figures 3 and 4 show the recorded strain traces from the bottom-left and bottom-right sensors, while Figures 5 and 6 show the same data from the top-left and top-right sensors. It should be noted that compressive strain has positive values and tensile strain, negative values on these graphs.

Analysing Figures 3 and 4, an immediate conclusion can be drawn that the signals recovered from the FBGs (pink traces) have lower amplitudes than those of the strain gauges. However, a closer examination reveals some discrepancies between the individual strain gauge records as well. Moreover, the traces in the negative strain regions around 0.2 to 0.3 s show a remarkably close match, especially in Figure 3. These similarities and discrepancies of the traces are very difficult to explain if the analysis is based on the current data alone.

On the other hand, Figures 5 and 6 reveal very significant differences between the recorded traces. Figure 5, especially, indicates measurement issues which are potentially attributed to some external influence, such as an error signal induced in the strain gauge wires due to the electromagnetic interference. It is unclear at present why the two strain gauge traces differ so much from one another and from the FBG record.

To shed more light on this, the readings of the “bottom” FBGs and the “top” FBGs are compared in Figures 7 and 8 respectively. Clearly, although the traces vary to some extent, the amplitudes are very similar for both the bottom and the top FBGs. This reinforces the argument of an erroneous strain gauge results in Figure 5.

It should be noted that the results obtained from Pulse 71990, representing a 164-ton plasma disruption, were representative of all the results recorded during the remaining pulses. However, in some cases, the differences between the magnitudes of the strain gauge and FBG signals were much greater than those presented in this paper, in other cases, the differences were smaller. The presentation and analysis of the complete set of results is beyond the scope of this paper.

2.4 Summary

The results of this small-scale trial have confirmed that the strain measurement system deployed on the vessel restraints in JET requires a further investigation to identify the causes of erroneous reporting by some sensors, especially those installed on the top restraints. Also, further investigation is required to understand the varying differences between the SG and FBG signal magnitudes recorded during different pulses.

The test has also demonstrated that an FBG-based measurement system is an attractive alternative to the foil strain gauges for determining the mechanical forces acting upon the vessel. The remaining part of this article will briefly assess the suitability of fibre Bragg grating technology for this purpose and highlight the engineering problems that need to be addressed before such as system can be deployed on JET.

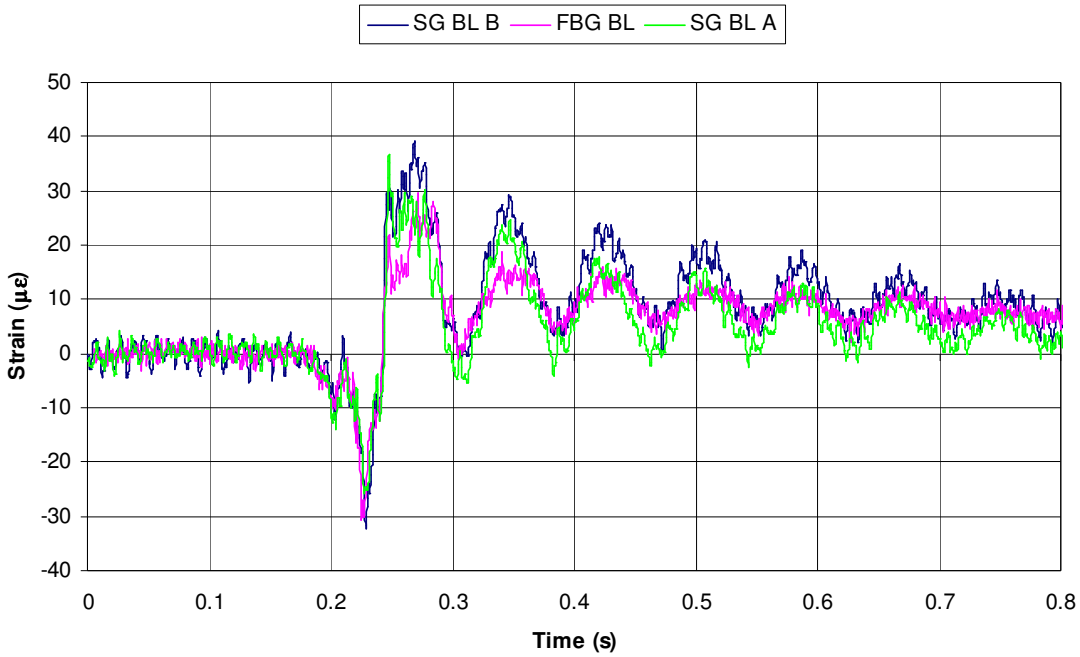

Figure 3. Plots of strain measurements derived from the originally mounted strain gauges (SG BL A and SG BL B) and an FBG (FBG BL). Note that "BL" stands for "bottom left".

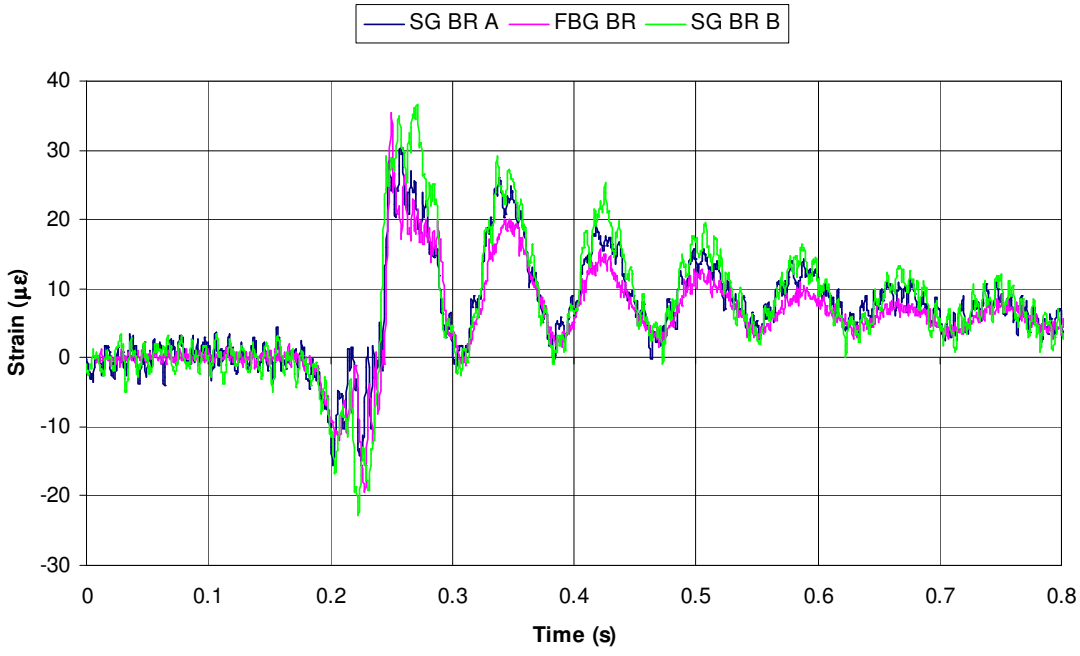

Figure 4. Plots of strain measurements derived from the originally mounted strain gauges (SG BR A and SG BR B) and an FBG (FBG BR). Note that "BR" stands for "bottom right".

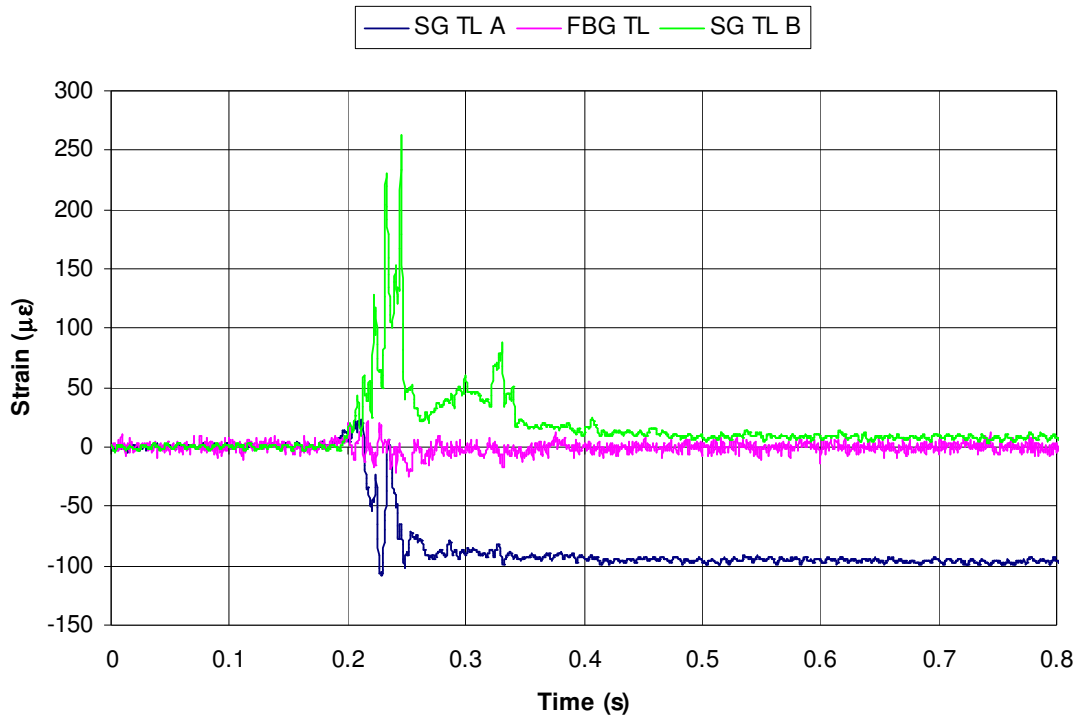

Figure 5. Plots of strain measurements derived from the originally mounted strain gauges (SG TL A and SG TL B) and an FBG (FBG TL). Note that "TL" stands for "top left".

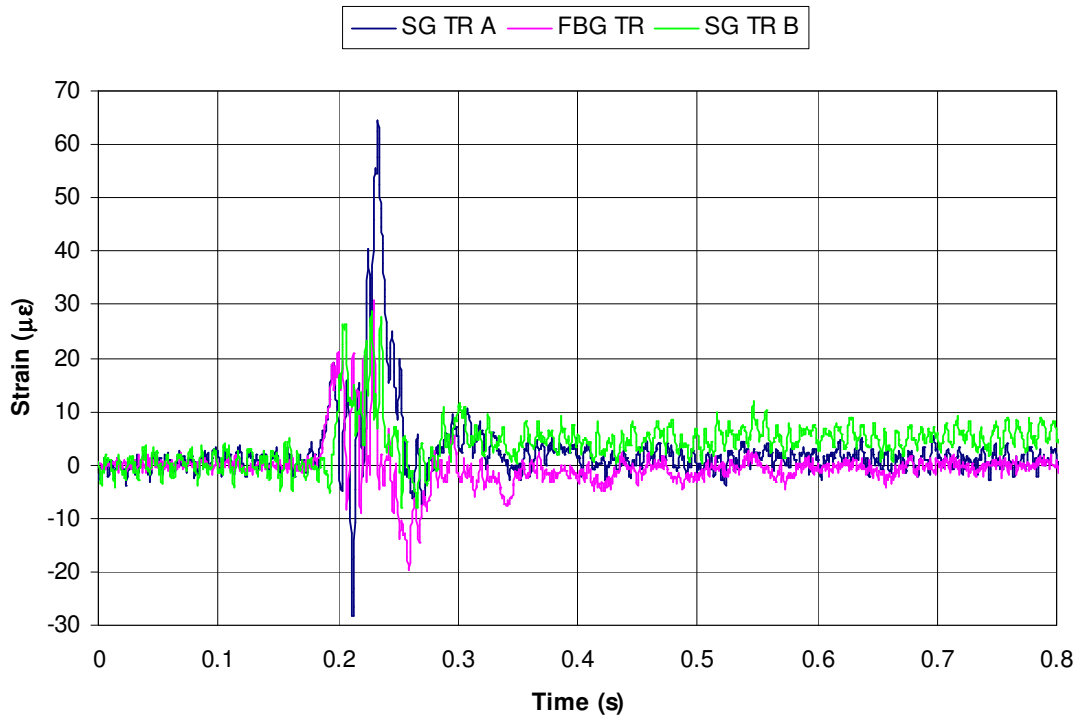

Figure 6. Plots of strain measurements derived from the originally mounted strain gauges (SG TR A and SG TR B) and an FBG (FBG TR). Note that "TR" stands for "top right".

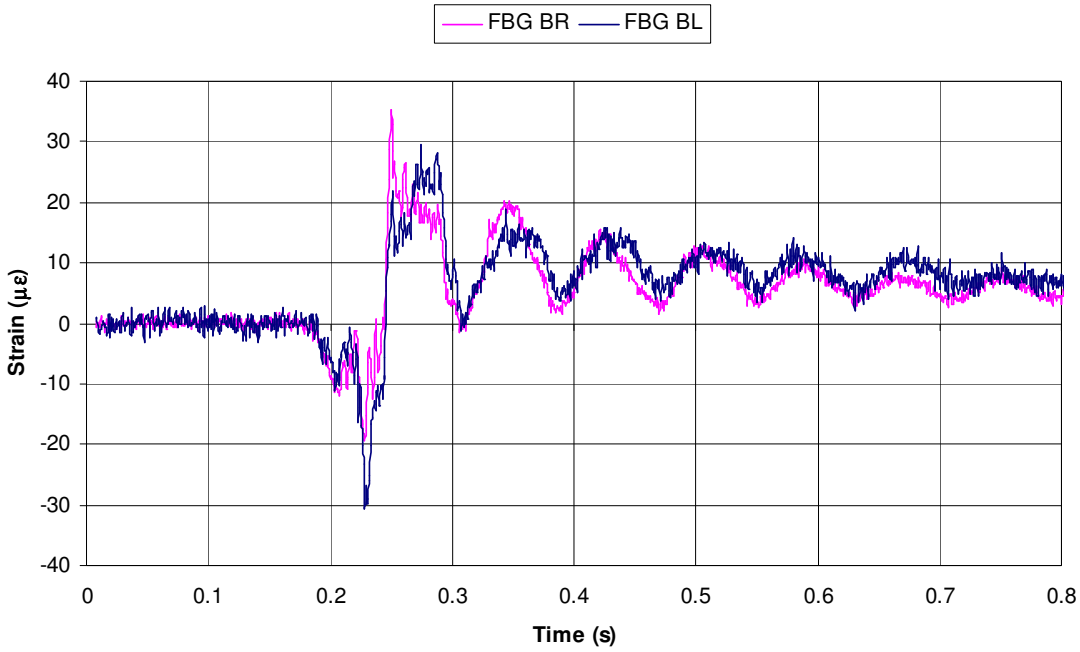

Figure 7. Comparison of strain readings from the "bottom" FBGs.

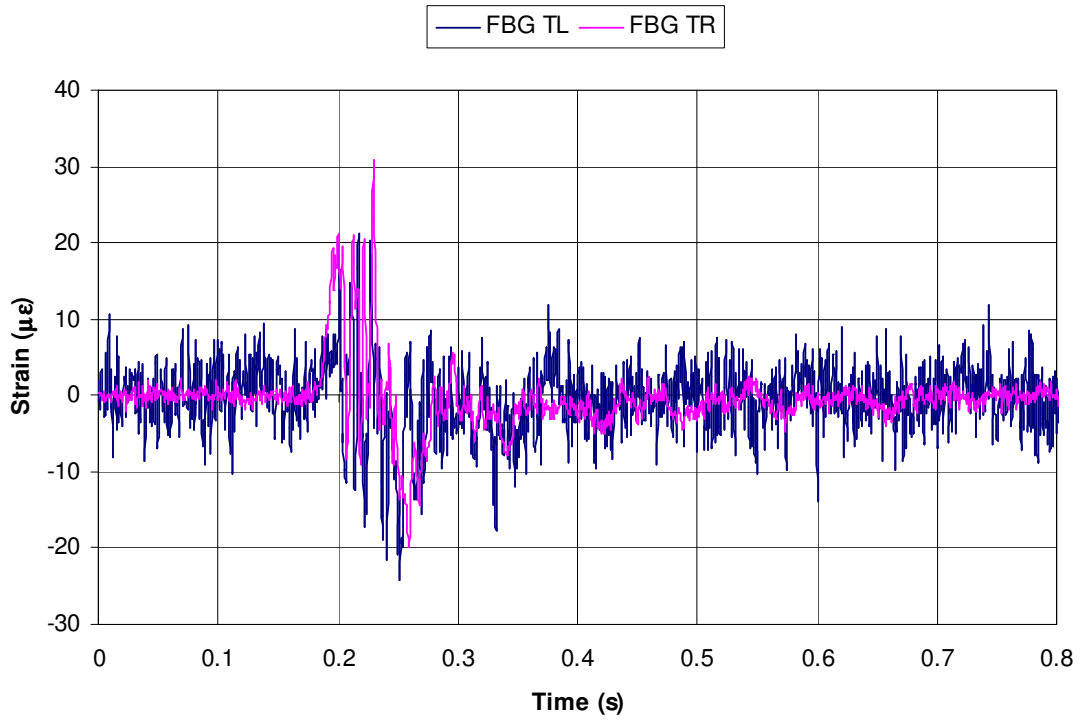

Figure 8. Comparison of strain readings from the "top" FBGs. (Note that BBG TL had a faulty splice and hence the noise level is increased.)

3. Proposal for the full-scale deployment

3.1 Functional, environmental and performance requirements

The deployment of a full-scale system to monitor all the supports of JET would require 32 (or indeed 64) sensors. The measurement range should be at least ±100 με to accommodate strain levels resulting from the largest disruptions, and the resolution should be better than ±2 με. For the dynamic measurements the system must enable a sampling rate equal to or greater than 2.5 kS/s, and for static measurements, the sampling rate should be at least 25 S/s. A continuous sampling is also required at 0.25 S/s, used to monitor the evolution of the forces on the leg during the bake out and the cool down phase of the Torus. This continuous data should be constantly recorded and available for display in JET control room. The measurement accuracy of the present strain gauge system on JET is unknown. However, it is desirable to ensure the highest level of accuracy achievable with the current state of the art in FBG sensing. Commercially available interrogators allowing 1 kS/s data acquisition offer up to 5 pm long-term stability, which is equivalent to approximately 4 με.

The operating temperature range of the sensors is between 20°C, when there is no operation, to approximately 80°C when the vessel is at its maximum temperature of 320°C. Such a temperature change would induce a peak wavelength shift equivalent to ~700 με; therefore, since the full-scale system will be required to measure both dynamic and static strains, temperature compensation will also be required.

The sensors must be able to perform under nuclear radiation conditions. An estimated neutron fluence for the operation in 2006 is 8×10^{12} n cm^{-2} – significantly lower than that reported in [3]. No data concerning the gamma radiation levels at the sensor locations are available at present.

3.2 Potential FBG-based measurement system configurations

Sensors

As highlighted above, temperature compensation will be required as the thermal error is nearly an order of magnitude larger than the strain measurement range. For the most accurate results, a temperature sensing array of secondary FBG sensors would have to be deployed alongside the primary strain sensing FBGs. Temperature sensors would have to be installed close to the strain sensors to achieve accurate compensation. In one approach, the temperature sensing FBGs could be decoupled mechanically from the monitored structure, for example, by placing them within a capillary tubing attached near to the strain sensing FBGs. An alternative, and possibly preferred, approach would be to align the secondary sensors perpendicularly to the primary sensors so that both types would react in the same way to the changing temperature whilst their strain responses would be opposite. Yet another solution would be to use two collocated gratings written in a single fibre length at the two significantly different wavelengths, e.g., 1300 nm and 1550 nm. Such gratings have different temperature and strain responses, and with further simple processing the two measurands could be separated.

Due to the large number of FBGs, their spectral separation will have to be optimised. It is desirable to devise an attachment method which would guarantee consistent peak shifts (or no shifts) due to the residual strain following the mounting process for all the

sensors. Care must be taken that individual FBG peaks will not overlap due to different thermal excursions or strains. Sensor mounting and protection similar to that developed for the small-scale trial could also be employed in the deployment of the full system.

Sensor network

Although the environment in which the system will be installed is hostile, the sensors can be accessed and replaced if necessary during machine shutdown. However, to minimise such undesirable interventions, it is proposed that a degree of redundancy is built in the sensor network. This can be achieved by doubling the entire system as in the case of the existing strain gauges. However, since temperature compensation will be required, a potentially more economical solution would be that highlighted above, i.e., the installation of two gratings per measurement point, one measuring axial and the other perpendicular strain. In this way, temperature compensation could be realised, whilst the system could also employ two separate lines to interrogate the axial and perpendicular sensors. To further improve fault tolerance, each of these lines could be subdivided into separate sections, each serving the top and the bottom sensors respectively. If one of the lines developed a fault or was damaged, then at least 75% of the sensors would remain operational. To still improve upon this result, the system could employ double ended interrogation, comprising optical switches. In the case of optical path failure at a single point, the sensor array would be interrogated from an end which serves a greater number of sensors. The deployment of military-grade fibre cable would ensure adequate mechanical strength.

Interrogation system

Depending on the functional and fault tolerance specifications, the system will have to be capable of interrogating between 32 and 64 sensors simultaneously at the rate of at least 2.5 kHz. To our knowledge, there are no commercially available systems meeting such challenging criteria.

One potential solution is to use a MEMS-based, electrostatically tunable Fabry-Perot filter to achieve this level of scanning rate for an entire C-band. In addition, data acquisition circuitry employed will have to be more powerful than that used in the present system. To take full advantage of the flexibility offered by digital signal processing and to minimise system nonlinearities [1], it would be desirable to realise FBG peak detection in software. A long-term stability of the system can be assured by the use of a wavelength reference, e.g., a gas cell.

To improve optical power budget and hence increase signal-to-noise ratio (SNR), the 3dB 50/50 optical coupler (shown in Figure 1) could be replaced with a 4-port optical circulator so that the incident light is redirected between ports instead of splitting it between two optical lines. By limiting the number of splices and connectors used for interconnecting the sensors, further optical power budget improvements would be achieved. Also, high power optical light sources such as ASE (Amplified Spontaneous Emission) could be employed to launch more optical power into the sensing lines and improve the SNR. A schematic diagram of a simplified system comprising 4 separate lines, with optional double-ended configuration indicated in line 4, is shown in Figure 9.

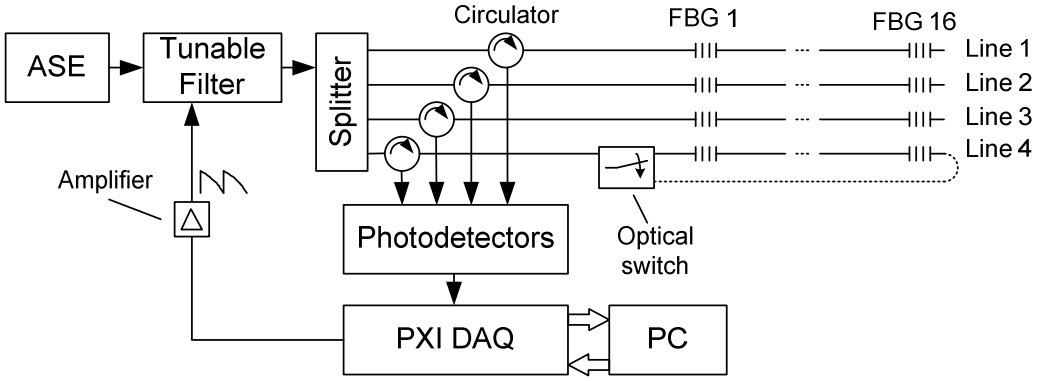

Figure 9. Potential configuration of a measurement system for the full-scale deployment on JET.

4. Conclusions

The results of the first-time demonstration of the FBG-based measurement system deployed on JET to measure dynamic forces in vessel restraints have been presented. The measurements derived from the FBGs mounted on the bottom two restraints of Octant 6 largely agree with the strain gauge data. However, the data from the top-left sensors show significant discrepancies. Further investigations are required to explain these discrepancies and also to understand the varying differences between the SG and FBG signal magnitudes recorded during different pulses, which could be due to electromagnetic interference. Furthermore, in the second part of this paper, we have presented an outline design of an optical measurement system for the full-scale deployment on JET. It is hoped that a similar system can be built and installed in the near future to improve our knowledge about the forces acting on the vacuum vessel during machine operation and to assist in the explanation of the phenomena highlighted above.

Acknowledgement

This work was carried out within the framework of the European Fusion Development Agreement. The views and opinions expressed herein do not necessarily reflect those of the European Commission.

References

1. G. Fusiek, P. Niewczas, J. R. McDonald, “Extended Step-out Length Fiber Bragg Grating Interrogation System for Condition Monitoring of Electrical Submersible Pumps”, Optical Engineering, Vol. 44, No. 3, pp 034404-1-10, March 2005
2. W. W. Morey, G. Meltz and W. H. Glenn, “Fibre optic Bragg grating sensors”. Proc. SPIE, vol. 1169, pp. 98-107, 1989
3. A. Fernandez Fernandez, A. I. Gusarov, B. Brichard *et al,* “Temperature monitoring nuclear reactor core with multiplexed fiber Bragg grating sensors”, Optical Engineering, Vol. 41, No. 6, pp 1246-1254, June 2002
4. A Fernandez Fernandez, A. I. Gusarov, B. Brichard *et al,* “Long-term radiation effects on fibre Bragg grating temperature sensors in a low flux nuclear reactor”, Measurement Science and Technology, Vol. 15, pp 1506-1511, 2004
5. M. Hughes, “Description of vessel support systems”, Machine Operations Group Documentation, UKAEA Fusion, Culham, December 2006
6. B. Brichard, “Implementation of optical fibres in diagnostic or inspection systems; Optical performance of a hydrogen-loaded optical fibre during the 2003 DT campaign”, JW0-FT-4.1, R-3933, SCK.CEN, Mol, Belgium, December 2004